

The Chiricahua Gap and the Role of Easterly Water Vapor Transport in Southeastern Arizona Monsoon Precipitation

F. MARTIN RALPH

Scripps Institution of Oceanography, University of California, San Diego, La Jolla, California

THOMAS J. GALARNEAU, JR.

Department of Hydrology and Atmospheric Sciences, The University of Arizona, Tucson, Arizona

(Manuscript received 24 February 2017, in final form 7 July 2017)

ABSTRACT

Between North America's Sierra Madre and Rocky Mountains exists a little-recognized terrain "gap." This study defines the gap, introduces the term "Chiricahua Gap," and documents the role of easterly transport of water vapor through the gap in modulating summer monsoon precipitation in southeastern Arizona. The gap is near the Arizona–New Mexico border north of Mexico and is approximately 250 km wide by 1 km deep. It is the lowest section along a 3000-km length of the Continental Divide from 16° to 45°N and represents 80% of the total cross-sectional area below 2.5 km MSL open to horizontal water vapor transport in that region. This study uses reanalyses and unique upper-air observations in a case study and a 15-yr climatology to show that 72% (76%) of the top-quartile (decile) monsoon precipitation days in southeast Arizona during 2002–16 occurred in conditions with easterly water vapor transport through the Chiricahua Gap on the previous day.

1. Introduction

The North American monsoon provides vital rainfall in the semiarid southwestern United States (Adams and Comrie 1997, and references therein). Occasionally, extreme rainfall and severe thunderstorm events occur in conjunction with the monsoon (e.g., Maddox et al. 1995; Adams and Souza 2009). In fact, analysis of 30 years of daily precipitation using rain gauges over the western United States showed that the top 10 rainfall days from over south-central California to eastern New Mexico mostly occurred during the summer monsoon season (Ralph et al. 2014). Despite the large body of published work on the North American monsoon, gaps remain in understanding, observations, weather predictions, and climate projections, particularly as it pertains to the transport of water vapor to the monsoon region.

Onset of the North American monsoon typically occurs as the continental anticyclone is established over the southwestern United States (e.g., Galarneau

et al. 2008), resulting in an easterly flow regime over much of New Mexico, Arizona, and southern California (e.g., Douglas et al. 1993). Much of the early work on the monsoon suggested that moistening of the environment over southern California, Arizona, and New Mexico west of the Continental Divide occurred in conjunction with easterly transport of water vapor from the Gulf of Mexico (Bryson and Lowry 1955; Reitan 1957; Sellers and Hill 1974). In contrast, later studies suggested instead that moisture originating west of the Continental Divide over the Gulf of California was responsible for the monsoon moistening below 700 hPa (e.g., Rasmusson 1967; Schmitz and Mullen 1996; Adams and Comrie 1997; Dominguez et al. 2016). The conceptual model for low-level southerly moisture surges in the Gulf of California was presented by Adams and Comrie (1997; their Fig. 4). These northward moisture surges have been linked to the passage of tropical easterly waves in the eastern North Pacific (Adams and Stensrud 2007) and the recurvature of tropical cyclones (Corbosiero et al. 2009). In this mechanism, the moisture initially surges northward to southern

Corresponding author: Thomas J. Galarneau, Jr., tgalarneau@email.arizona.edu

California and southwest Arizona, then turns eastward and moves into southeast Arizona. Conversely, Adams and Comrie (1997) argued that low- to mid-level moisture transported westward from the east side of the Continental Divide is inhibited substantially by drying in downslope flow on the west side of the Sierra Madre. It was recognized that moisture originating from the Gulf of Mexico region may still be important for moistening the environment, but primarily above 700 hPa.

These earlier results formed the background for analysis of unique observations of vertical profiles of winds aloft collected during the 2009 and 2010 monsoon seasons (defined here as 1 July–1 October) in southeast Arizona. The data enabled evaluation of the water vapor transport pathways during these summers. The data are from a wind profiling radar that was located near Tucson, Arizona (see location of “PAP” in Fig. 1b). This wind profiler was operated by the National Oceanic and Atmospheric Administration (NOAA)/Earth System Research Laboratory and was utilized for U.S. Army parachutist training. Examination of the wind profiler observations for select heavy rainfall events during these monsoon seasons showed that flow was easterly throughout a deep layer for almost all the cases (a representative case study is shown below). This result suggested that water vapor transport from the east side of the Continental Divide may play an important role in monsoon rainfall over southeast Arizona, even though the most recent key studies had concluded that water vapor transport into the region was primarily from the southwest with the caveat that many of these studies examined the core of the monsoon region over northwest Mexico rather than southeast Arizona.

Given the observation that heavy monsoon rains in 2009 and 2010 were accompanied by deep easterly flow, a key aim of this paper is to test the hypothesis that easterly moisture transport from the east side of the Continental Divide plays an important role in North American monsoon rainfall in southeast Arizona. A close examination of the terrain east of southeastern Arizona revealed a low point, or “gap,” in the Continental Divide through which enhanced westward (easterly) water vapor transport could occur. The remainder of this paper is organized as follows. Section 2 describes (and names) this gap in the Continental Divide. Section 3 introduces the key datasets and analysis methods. Section 4 describes the results from a case study of the heavy monsoon rain event of 13–14 August 2009 and a climatology of water vapor transport and precipitation for the

2002–16 monsoon seasons. Conclusions are presented in section 5.

2. Identification of the Chiricahua Gap

These preliminary analyses led to a closer look at the terrain east of the region. The Intermountain West is characterized by complex terrain features associated with the Rocky Mountains of the United States and the Sierra Madre of Mexico (Fig. 1a). Close inspection of the Arizona, New Mexico, and Mexico intersection reveals the presence of a terrain gap extending from extreme northern Mexico to just west of Silver City, New Mexico (SVC; Fig. 1b). This terrain gap is approximately 250 km across and 1 km deep, and it represents the lowest section of the Continental Divide between 16° and 45°N (Fig. 1c). Neither the authors nor the U.S. Board on Geographic Names were able to identify a preexisting name for this gap, and thus the name “Chiricahua Gap” is introduced here. This reflects both the name of a nearby mountain range in southeast Arizona (Figs. 1b,c) and the region’s Native American history. The Chiricahua Gap represents 80% of the total cross-sectional area below 2.5 km above mean sea level (MSL) open to horizontal water vapor transport along the Continental Divide between 16° and 45°N (Fig. 1d).

3. Hydrometeorological data and methods

The Climate Forecast System Reanalysis (CFSR; Saha et al. 2010, 2014) dataset is available four times daily at $0.5^\circ \times 0.5^\circ$ horizontal grid spacing on isobaric levels at 50-hPa increments (25 hPa below 750 hPa and between 100 and 250 hPa) and constitutes the primary data source for the case study and climatology. Precipitation analyses utilize the National Centers for Environmental Prediction (NCEP) Stage IV gridded precipitation dataset (Lin 2011), available at 4-km horizontal grid spacing. Upper-air observations from the radiosonde station located at the Tucson, Arizona (TWC), NOAA/National Weather Service (NWS) Office and the NOAA wind profiling radar that was located at the U.S. Army Parachute Test and Training Facility in Tucson, Arizona (PAP), during 2009–10, are utilized for the case study analysis (Fig. 1b). A comparison of the PAP wind observations and the CFSR wind field for 13 August 2009 is shown in Fig. 2. Overall, the CFSR is able to represent the transient circulation features depicted in the PAP wind observations, including an important deep easterly flow maximum at 1200 UTC 13 August that will be discussed in the case study analysis in section 4.

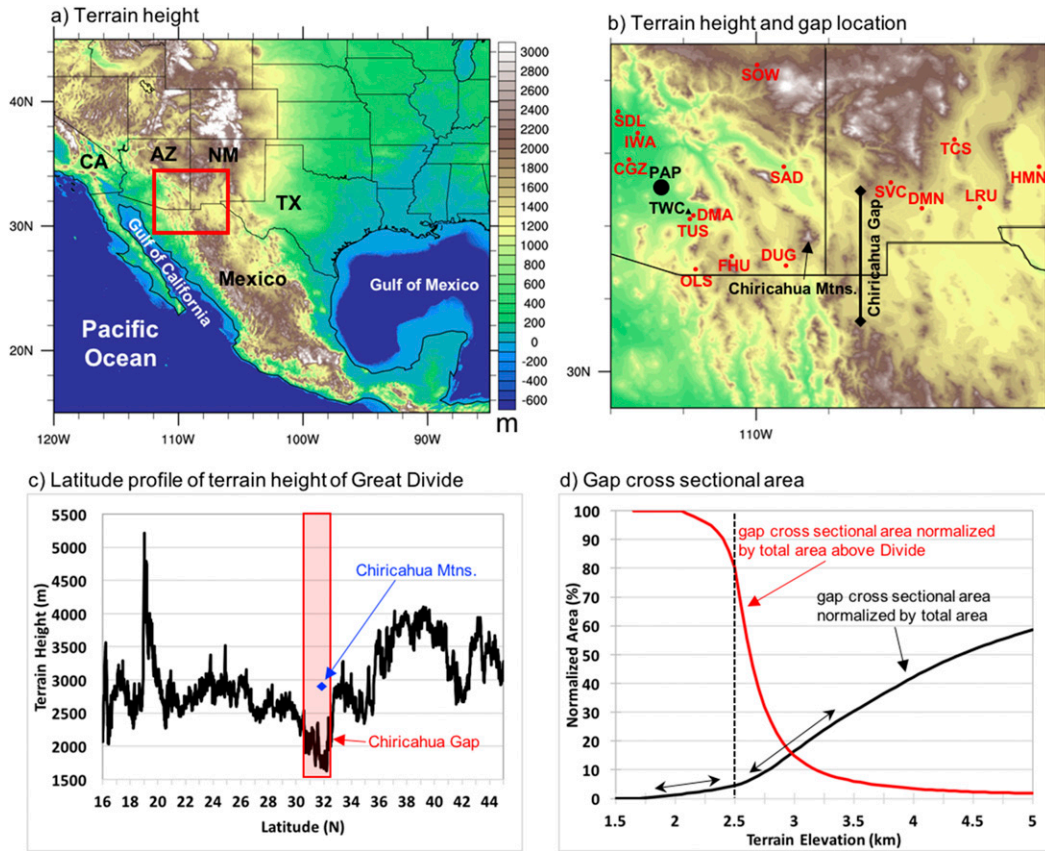


FIG. 1. Terrain height and bathymetry (shaded; m) over much of the (a) continental United States and Mexico and (b) southern Arizona and New Mexico and northern Mexico. The area shown in (b) is indicated by the red box in (a). In (b), the location of selected Automated Surface Observing Stations (ASOS) are labeled in red, and PAP and TWC are labeled in black. The Chiricahua Mountains and Gap are also labeled. (c) Latitude profile of the height (m) of the Continental Divide. The height of the Chiricahua Mountains is labeled by the blue diamond. The meridional extent of the Chiricahua Gap is marked by the red box. (d) Fraction of area of the Continental Divide that is open to zonal water vapor transport (black line; %) and fraction of total flow that is occupied by the Chiricahua Gap (red line; %) as a function of terrain elevation (km). This figure is derived from the NOAA/National Centers for Environmental Information ETOPO1 1-arc-min global relief model (Amante and Eakins 2009).

This comparison provides confidence in the ability of the CFSR to capture key sub-synoptic-scale circulation features in southeast Arizona and near the Chiricahua Gap.

The vertically integrated water vapor transport (IVT) is computed to diagnose the water vapor transport through the Chiricahua Gap during the active monsoon period (defined here as 1 July–1 October) in 2002–16. The IVT is calculated following the method of Moore et al. (2012):

$$IVT = - \int_{p_0}^p (q\mathbf{V}) \frac{dp}{g}, \quad (1)$$

where p_0 is 1000 hPa, p is 300 hPa, \mathbf{V} is the horizontal wind vector, q is the specific humidity, and

g is the acceleration due to gravity. Grid point data that are located on pressure levels considered below ground are masked prior to the computation of IVT.

The area-mean daily rainfall for southeast Arizona during the 2002–16 monsoon seasons was computed using the NCEP Stage IV dataset, with a “day” defined as the 24-h period ending at 1200 UTC and for the area covering 31°–33°N and 111.5°–109°W. The distribution of southeast Arizona area-mean rainfall in 2002–16 is shown in Fig. 3. We define monsoon “bursts” as the upper quartile of days with area-mean rainfall ≥ 2.6 mm. Heavy bursts are defined as the 90th percentile of days with area-mean rainfall ≥ 4.5 mm, and moderate bursts with 2.6–4.5 mm of area-mean rainfall.

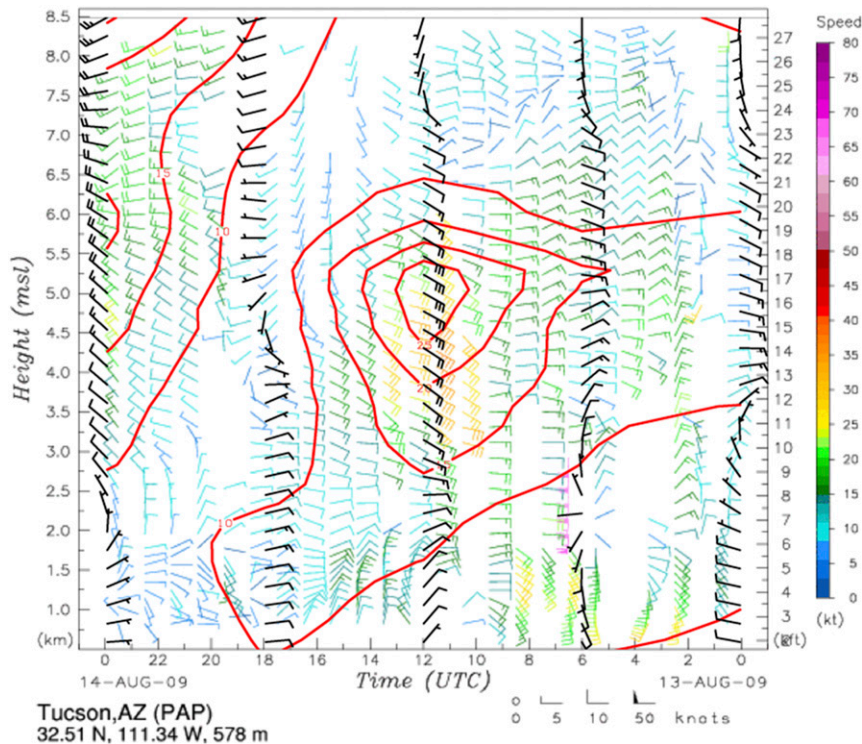


FIG. 2. Time (UTC)–height (km MSL) section of NOAA profiler wind (bars as indicated in the key and color coded by magnitude according to the color bar; kt, where $1 \text{ kt} = 0.51 \text{ m s}^{-1}$) observations for PAP and CFSR vector wind (black bars; kt) and wind speed (red contours every 5 kt starting at 10 kt) at 32.5°N , 111.5°W , at 0000 UTC 13–14 Aug 2009. The base image of PAP profiler winds was obtained from the NOAA/Earth System Research Laboratory.

4. Results

a. Heavy monsoon burst on 13–14 August 2009

A heavy monsoon burst occurred over southeast Arizona on 13–14 August 2009, with daily area-average rainfall amounts of 4.78 mm ending at 1200 UTC 13 August and 7.65 mm at 1200 UTC 14 August 2009 representing the largest rainfall event over southeast Arizona during the 2009 monsoon season (Fig. 4a). The map of rainfall for the 48-h period ending at 1200 UTC 14 August 2009 shows a widespread region of $\geq 16 \text{ mm}$ over much of southeast Arizona, with amounts over 32 mm in far southeast Arizona (Fig. 4b). These rainfall amounts exceeded 50% of the total August 2009 rainfall over large regions south and east of Tucson, Arizona. Examination of the radiosonde observations at TWC shows a moist 600–450-hPa layer collocated with easterly flow on 1200 UTC 12 August (Fig. 5a). By 0000 UTC 13 August, the easterly flow increased to near 10 m s^{-1} in the moist layer, with warm air advection present above 500 hPa associated with an upper-level trough to the west (Fig. 5b). Between 0000

and 1200 UTC 13 August, the low-level moisture increased as the easterly flow deepened to just above the surface with a corresponding 60% increase in total column precipitable water (PW) from 25 to 40 mm at TWC by 1200 UTC 13 August (Fig. 5c). The hourly PAP wind profiler observations confirm the deepening easterly flow between 0000 and 1200 UTC 13 August (Fig. 2). The flow was consistently easterly between 2 and 8 km MSL throughout 13 August, reaching nearly 18 m s^{-1} in the 3–6 km MSL layer by 1200 UTC. Below 2 km MSL, however, the flow was more southerly and southeasterly during that time, eventually shifting to northerly after 1200 UTC. By 1800 UTC 13 August, the westerlies deepened as the upper-level trough to the west progressed eastward (Fig. 5d).

Analysis of zonal IVT in the Chiricahua Gap shows that the increase in PW over southeast Arizona occurred during a period of easterly IVT (Fig. 4a). The easterly IVT is located on the north side of a mesoscale vortex located over northern Mexico near the Arizona–New Mexico border and the southwest side of an anticyclone centered over eastern New Mexico at 0600

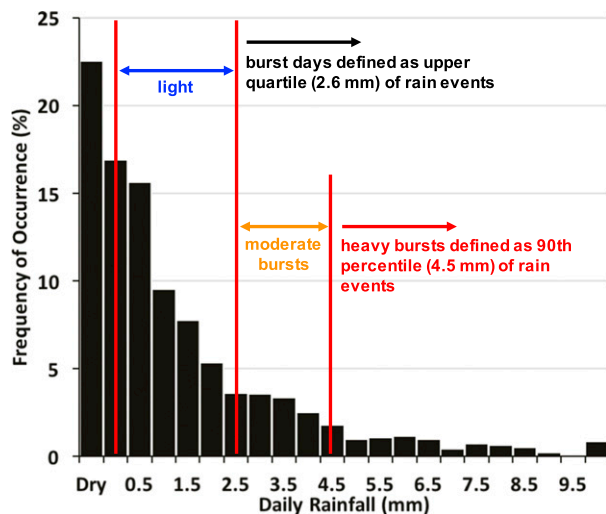


FIG. 3. Histogram of area-average daily rainfall (mm) over southeast Arizona during the 2002–16 monsoon seasons. The geographical area used for the averaging is depicted in Fig. 6a and described in the text.

UTC 13 August (Fig. 6a). Manual tracking of the mesoscale vortex suggests that it originated in conjunction with an organized mesoscale convective complex (MCC; Maddox 1980) over the high terrain of central Mexico (not shown) that formed on the northeast flank of an inverted trough located over the Gulf of California at 0600 UTC 13 August (Fig. 6a). The inverted trough is similar to those documented by Douglas and Englehart (2007) during the 2004 North American Monsoon Experiment (Higgins et al. 2006). A meridional cross section through the Chiricahua Gap at 0600 UTC 13 August shows that the strongest easterly IVT was located below 700 hPa on the north side of the mesoscale vortex within the Gap (Fig. 6b). By 1200 UTC 13 August, the mesoscale vortex had moved north-northeastward to near the Arizona–Mexico border (not shown), contributing to an increase in easterly flow near 4–5 km MSL at PAP by 1200 UTC.

b. Climatology of IVT in Chiricahua Gap and southeast Arizona monsoon bursts in 2002–16

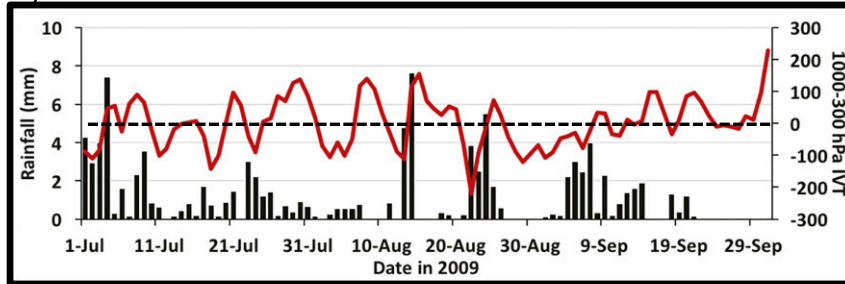
Analysis of the 13–14 August 2009 heavy monsoon burst in southeast Arizona highlighted the importance of easterly water vapor transport through the Chiricahua Gap in moistening the environment, thereby contributing to the heavy rains. The question arises as to how general the results are from a single brief case study. To address this issue, a climatology was constructed of area-average rainfall over southeast Arizona and zonal IVT in the Chiricahua Gap (area-averaging regions are

shown in Fig. 6a) for the 2002–16 summer monsoon seasons. As with the previous analyses, a day is defined as the 24-h period ending at 1200 UTC. Daily rainfall over southeast Arizona (day –0) is compared with the zonal IVT in the Chiricahua Gap on the previous day (day –1), which establishes a cleaner relationship between the two variables and is physically meaningful since it should be expected that easterly IVT on day –1 will help moisten southeast Arizona for rainfall the following day.

Figure 7a shows a scatterplot of zonal IVT on day –1 versus total rainfall on day –0 for all days in which rainfall occurred over southeast Arizona in the 2002–16 summer monsoon seasons. The results show that 58% (489 out of 847) of light rain events occur with easterly IVT. The preference for easterly IVT increases with stronger events, as 69% (118 out of 170) of moderate and 76% (86 out of 113) of heavy rain events have easterly IVT. The distribution of IVT for all summer monsoon days in 2002–16 shows that only 39% (109 out of 278) of dry days have easterly IVT (Fig. 7b). This result is in stark contrast to the distribution for all rain days, and especially heavy burst days, where there is a clear preference for easterly IVT. To account for some minor skewness to the distributions, the nonparametric Wilcoxon–Mann–Whitney rank sum test (Wilks 1995, 138–143) was used to assess significance. The confidence for rejecting the null hypothesis exceeded 95% when comparing heavy, moderate, or light events with dry days, and heavy with light events. These robust results show clearly how easterly IVT is a definitive characteristic of the heavy burst rain events during the summer monsoon in southeast Arizona.

To determine the synoptic-scale flow structure of the heavy burst days with easterly IVT in the Chiricahua Gap, a composite analysis of heavy burst days with IVT anomalies ≤ -1.0 standard deviation σ (compared to the 2002–16 climatology) is constructed (Fig. 8a). The composite at day –1 shows that 1) PW anomalies exceed $+1.0\sigma$ (relative to the 1979–2016 long-term climatology) over much of northern Mexico, eastern Arizona, and southwest New Mexico and 2) southeasterly IVT anomalies are present over the Chiricahua Gap region on the northeast flank of a cyclonic circulation feature in northwest Mexico characterized by streamfunction anomalies near -1.0σ . This composite resembles the synoptic-scale flow pattern for the 13–14 August 2009 case, suggesting that cyclonic circulation features over northern Mexico are key to driving easterly IVT through the Chiricahua Gap. This cyclonic circulation in the composite is likely composed of inverted trough, easterly wave,

a) Time series of rainfall and zonal IVT in 2009



b) 13–14 Aug 2009 total rain and % of month

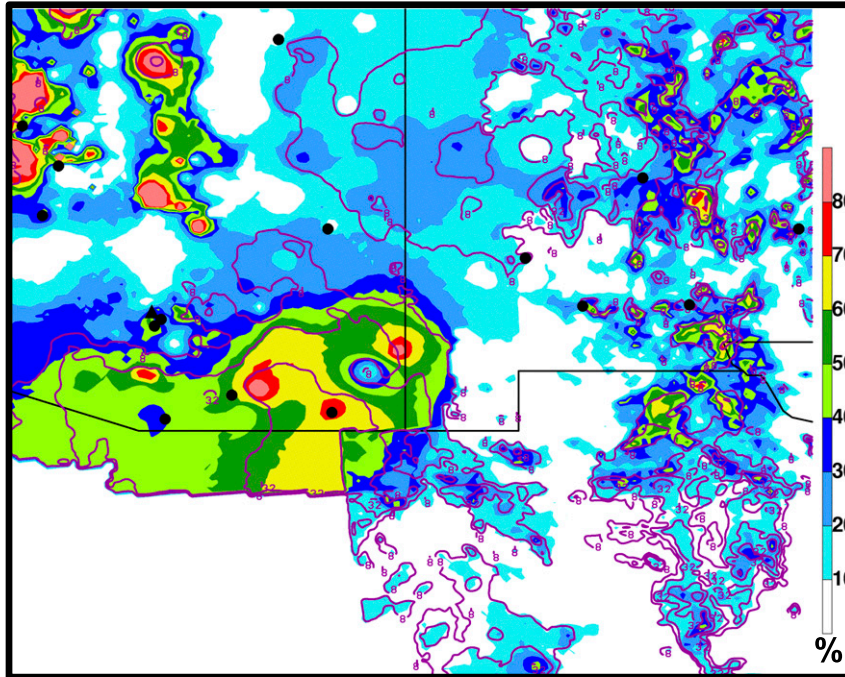


FIG. 4. Time series of area-average daily rainfall (black bars; mm) over southeast Arizona and area-average zonal IVT in the Chiricahua Gap (red line; $\text{kg m}^{-1} \text{s}^{-1}$) from 1 Jul to 1 Oct 2009. The geographical areas used for the averaging are depicted in Fig. 6a. (b) Stage-IV accumulated rainfall (purple contours at 8, 16, 32, 64, and 128 mm) and percent of total August 2009 rainfall (shaded; %) for 48-h period ending 1200 UTC 14 Aug 2009. The ASOS stations from Fig. 1b are labeled with filled black circles.

and mesoscale convective vortex cases generated over northern Mexico. The spatial distribution of daily mean rainfall for the heavy burst composite shows that the heaviest rains occur over far southeast Arizona by definition, but also extends north and northwestward across Arizona (Fig. 8b). The subset of heavy burst events represents up to 18% of the total annual monsoon rains across the region, demonstrating that the impact of easterly IVT in the Chiricahua Gap on daily rainfall extends beyond the southeast Arizona region.

The same composite is constructed for dry days in southeast Arizona for comparison (Fig. 8c). Interestingly,

for dry days in which easterly IVT $\leq -1.0\sigma$ was present in the Chiricahua Gap, the synoptic-scale flow pattern is characterized by a weak cyclonic circulation feature near the Gulf of California and an anomalous anticyclonic circulation centered over Colorado and New Mexico (Fig. 8c). The key difference between the dry and heavy burst days is the dominance of the anticyclone and the overall reduced PW throughout the region in the dry composite. The IVT vectors are also more easterly in the dry composite compared to southeasterly in the heavy burst composite (Figs. 8a,c), suggesting that moisture transport from the Gulf of Mexico and northeast Mexico does not occur

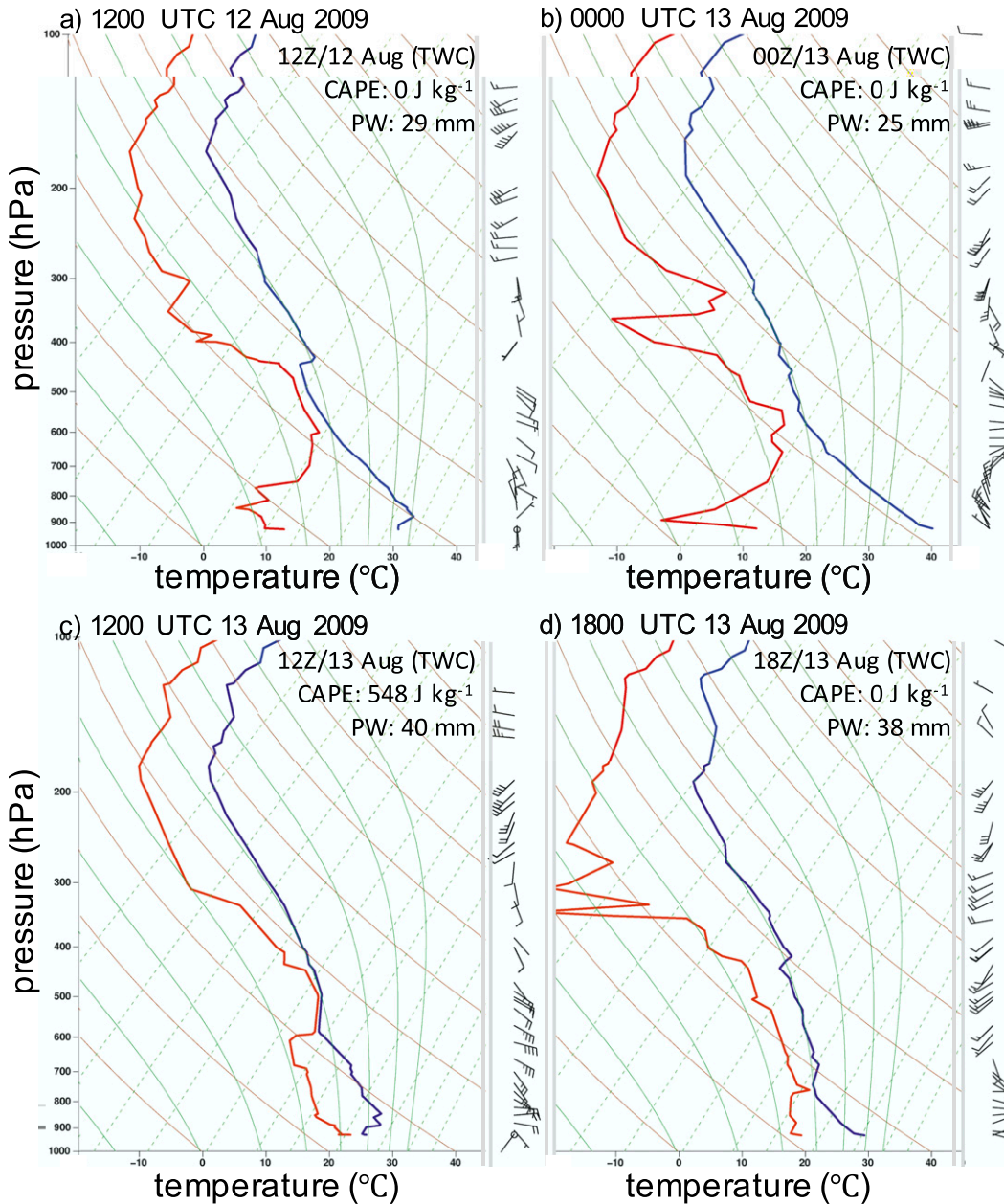


FIG. 5. Skew T - $\log p$ diagrams using data from radiosondes launched from TWC show air temperature ($^{\circ}\text{C}$; blue), dewpoint ($^{\circ}\text{C}$; red), and vector wind (half barb = 2.5 m s^{-1} , full barb = 5.0 m s^{-1}) at (a) 1200 UTC 12 Aug, (b) 0000 UTC 13 Aug, (c) 1200 UTC 13 Aug, and (d) 1800 UTC 13 Aug 2009. The convective available potential energy (J kg^{-1}) and PW (mm) are indicated.

in situations where the anticyclone is located over northwest New Mexico.

5. Conclusions

This study introduced the Chiricahua Gap, which is an orographic feature along the Continental Divide in southwest New Mexico that is important to southeastern

Arizona monsoon precipitation, and potentially to southwestern U.S. weather and climate in general. The name of this terrain gap is derived from the nearby Chiricahua Mountains in southeast Arizona and reflects the region’s Native American heritage. Analysis of a heavy monsoon burst on 13–14 August 2009 and a climatology of the 2002–16 summer monsoon seasons showed that easterly water vapor transport through the

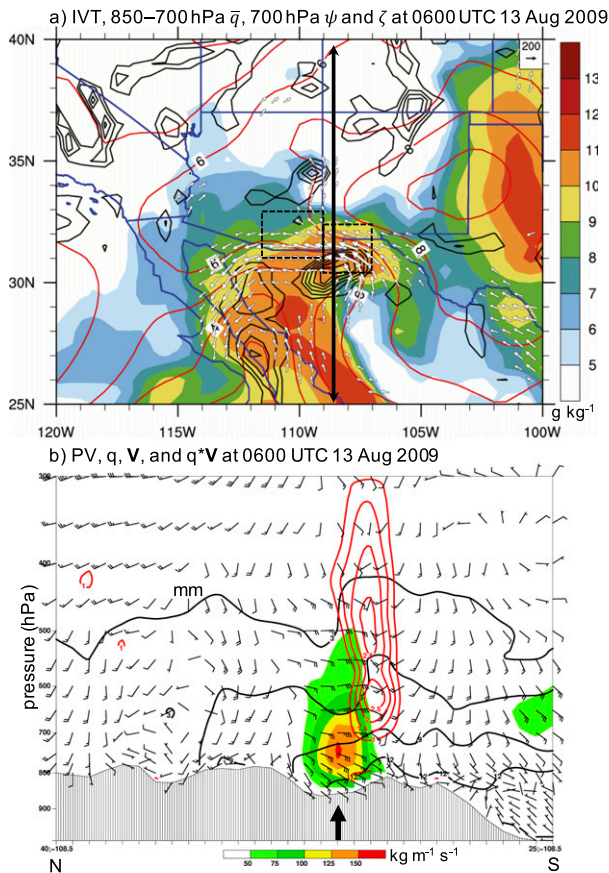


FIG. 6. (a) The 700-hPa streamfunction (red contours every $1.0 \times 10^6 \text{ m}^2 \text{ s}^{-1}$), 700-hPa relative vorticity (black contours every $4.0 \times 10^{-5} \text{ s}^{-1}$ starting at $4.0 \times 10^{-5} \text{ s}^{-1}$), 850–700-hPa layer-mean specific humidity (shaded; g kg^{-1}), and IVT (arrows; $\text{kg m}^{-1} \text{ s}^{-1}$). (b) Vertical cross section of vector wind (half barb = 2.5 m s^{-1} , full barb = 5.0 m s^{-1}), water vapor mixing ratio (black contours every 3 g kg^{-1} starting at 3 g kg^{-1}), potential vorticity [red contours every 0.5 potential vorticity units (PVU), where $1.0 \text{ PVU} = 1.0 \times 10^{-6} \text{ m}^2 \text{ s}^{-1} \text{ K kg}^{-1}$, starting at 1.0 PVU], and easterly IVT magnitude (shaded according to the color bar; $\text{kg m}^{-1} \text{ s}^{-1}$) at 0600 UTC 13 Aug 2009. In (a), the averaging areas for southeast Arizona and Chiricahua Gap region are indicated by black dashed boxes, and the vertical cross-section orientation is indicated by a black arrow. In (b), the location of the Chiricahua Gap is marked by a black arrow.

Chiricahua Gap (on the day *before* heavy precipitation) is a definitive characteristic of the wettest monsoon days in southeast Arizona. Thus, the ability to predict easterly IVT in the Chiricahua Gap is a key component to accurately predicting the wettest summer monsoon days in the region. This result is analogous to findings involving the key role of low-altitude water vapor transport in atmospheric rivers over the Pacific Ocean (and elsewhere globally) in extreme precipitation on the U.S. West Coast (and other mid-latitude west coasts; e.g., Ralph et al. 2006, 2016; Lavers et al. 2016).

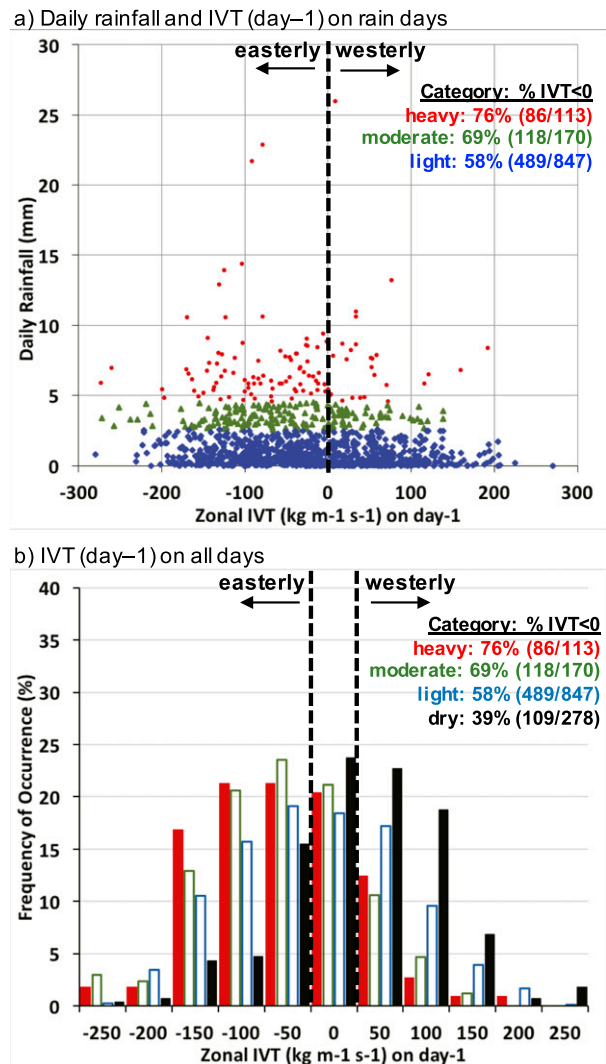


FIG. 7. (a) Scatterplot of area-average zonal IVT ($\text{kg m}^{-1} \text{ s}^{-1}$) in Chiricahua Gap on day -1 vs area-average daily rainfall (mm) over southeast Arizona on day -0. Heavy, moderate, and light events are marked by red-filled circles, green-filled triangles, and blue-filled diamonds, respectively. (b) Histogram of area-average zonal IVT ($\text{kg m}^{-1} \text{ s}^{-1}$) in the Chiricahua Gap on day -1 for heavy (red), moderate (green), light (blue), and dry days (black). This climatology is for the summer monsoon seasons in 2002–16. In both panels, the zero zonal IVT value is marked by the vertical black dashed line and the statistics are summarized in the key.

The results from this study differ from previous studies on the North American monsoon (since the 1970s), which emphasized the importance of southwesterly moisture surges originating in the Gulf of California in the occurrence of rainfall over southern Arizona and northwest Mexico (e.g., Schmitz and Mullen 1996; Adams and Comrie 1997; Dominguez et al. 2016). It has been argued that while moisture above

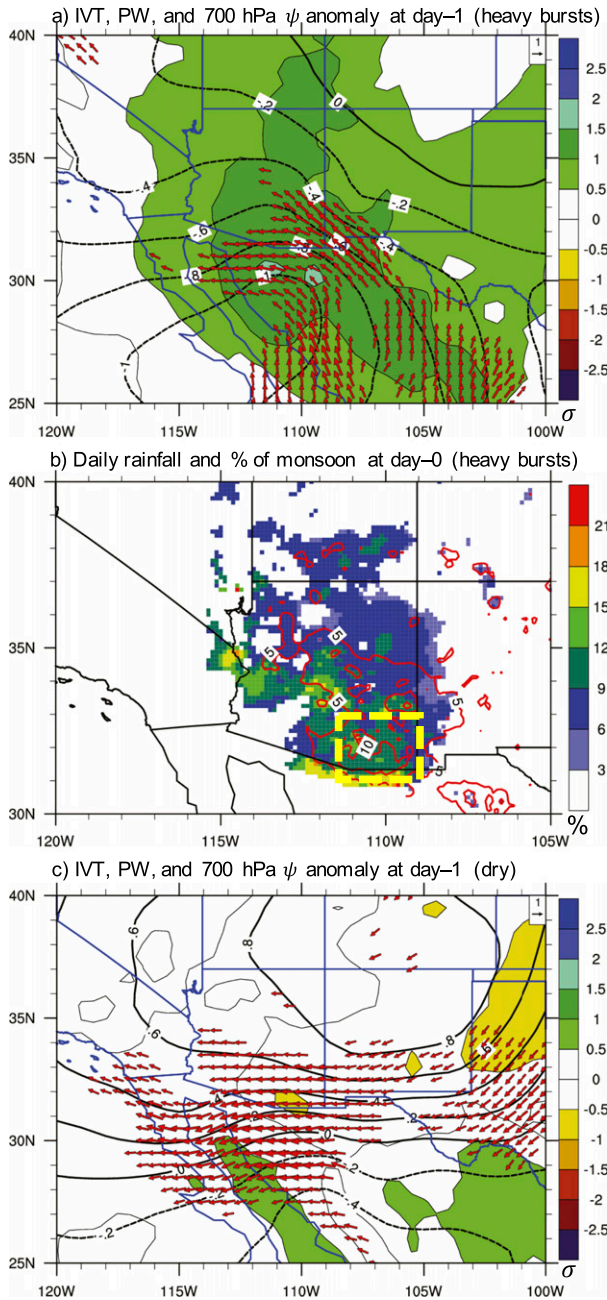


FIG. 8. Composite mean of standardized anomalies (relative to the long-term 1979–2016 climatology) of IVT (arrows $\geq 1.0\sigma$), PW (shaded according to the color bar; σ), and 700-hPa streamfunction (contours every 0.2σ ; negative dashed; positive solid) at day -1 for (a) heavy bursts ($n = 29$) and (c) dry days ($n = 21$) with area-average zonal IVT anomaly $\leq -1.0\sigma$ (relative to the 1 Jul–1 Oct 2002–16 climatology) in the Chiricahua Gap. (b) Composite mean daily rainfall (red contours every 5 mm starting at 5 mm) and percent of annual summer monsoon rainfall (shaded according to the color bar; %) for heavy burst days with area-average zonal IVT anomaly $\leq -1.0\sigma$ (relative to the 1 Jul–1 Oct 2002–16 climatology) in the Chiricahua Gap. The percent of annual summer monsoon rainfall is shaded where differences in daily rainfall for heavy burst days and the 1 Jul–1 Oct 2002–16 climatology are statistically significant at the 99.9% confidence level using a Student’s t test. In (b), the averaging area for southeast Arizona rainfall is indicated by yellow dashed box.

700 hPa originating from the east side of the Continental Divide may be important for summer monsoon rainfall, low-level moisture below 700 hPa originates from the Gulf of California. The results presented herein, however, show that low-altitude moisture during the heavy burst summer monsoon events over southeast Arizona, which is located on the eastern periphery of the North American monsoon region, originates significantly from the east side of the Continental Divide from northern Mexico and the Gulf of Mexico. While previous studies have shown that water vapor from the east side of the Continental Divide can contribute to summer monsoon rainfall (e.g., Bosilovich et al. 2003; Hu and Dominguez 2015), the present study is unique in that it identifies the Chiricahua Gap and shows how the Gap allows low-altitude moisture below 700 hPa to pass through the Continental Divide and into southeast Arizona. This behavior is most prevalent for the heaviest rainfall days in southeast Arizona during the summer monsoon.

Future and ongoing research will aim to compare summer monsoon rainfall and IVT over southeast Arizona with southwest Arizona, southern California, and northwest Mexico. These future analyses will also employ key surface observation stations and the SuomiNet Global Positioning System PW observations (Ware et al. 2000). Additionally, a Lagrangian perspective will be used to determine the source region of the water vapor on the east side of the Continental Divide. Numerical modeling experiments must be conducted to explore the relevant physical and dynamical processes that drive heavy rainfall over southeast Arizona during the monsoon. Convective-resolving simulations with horizontal grid spacing < 3 km will allow for detailed examination of airflow in and near the Chiricahua Gap, and sensitivity experiments with altered configurations of the Gap may provide more insight on the Gap’s importance in water vapor transport. Finally, ensemble-based sensitivity techniques (e.g., Torn and Hakim 2008) can be used to quantitatively demonstrate the sensitivity of rainfall over southeast Arizona to water vapor transport through the Chiricahua Gap during the summer monsoon. This ensemble sensitivity analysis technique has been successfully used in previous studies to quantitatively examine how synoptic-scale circulation features and water vapor transport can impact organized convection and rainfall over the southern plains (Torn et al. 2017).

Acknowledgments. Research support was provided by the Scripps Institution of Oceanography (Ralph) and the University of Arizona Office for Research and Discovery (Galarneau). This study benefitted from

discussions with Jason Cordeira. Three anonymous reviewers are thanked for their insightful comments and suggestions that helped to improve the paper.

REFERENCES

- Adams, D. K., and A. C. Comrie, 1997: The North American Monsoon. *Bull. Amer. Meteor. Soc.*, **78**, 2197–2213, doi:10.1175/1520-0477(1997)078<2197:TNAM>2.0.CO;2.
- , and E. P. Souza, 2009: CAPE and convective events in the southwest during the North American monsoon. *Mon. Wea. Rev.*, **137**, 83–98, doi:10.1175/2008MWR2502.1.
- Adams, J. L., and D. J. Stensrud, 2007: Impact of tropical easterly waves on the North American monsoon. *J. Climate*, **20**, 1219–1238, doi:10.1175/JCLI4071.1.
- Amante, C., and B. W. Eakins, 2009: ETOPO1 1 arc-minute global relief model: Procedures, data sources, and analysis. NOAA Tech. Memo. NESDIS NGDC-24, 25 pp. [Available online at <https://www.ngdc.noaa.gov/mgg/global/relief/ETOPO1/docs/ETOPO1.pdf>.]
- Bosilovich, M. G., Y. C. Sud, S. D. Schubert, and G. K. Walker, 2003: Numerical simulation of the large-scale North American monsoon water sources. *J. Geophys. Res.*, **108**, 8614, doi:10.1029/2002JD003095.
- Bryson, R., and W. P. Lowry, 1955: Synoptic climatology of the Arizona summer precipitation singularity. *Bull. Amer. Meteor. Soc.*, **36**, 329–339.
- Corbosiero, K. L., M. J. Dickinson, and L. F. Bosart, 2009: The contribution of eastern North Pacific tropical cyclones to the rainfall climatology of the southwest United States. *Mon. Wea. Rev.*, **137**, 2415–2435, doi:10.1175/2009MWR2768.1.
- Dominguez, F., G. Miguez-Macho, and H. Hu, 2016: WRF with water vapor tracers: A study of moisture sources for the North American monsoon. *J. Hydrometeor.*, **17**, 1915–1927, doi:10.1175/JHM-D-15-0221.1.
- Douglas, A. V., and P. J. Englehart, 2007: A climatological perspective of transient synoptic features during NAME 2004. *J. Climate*, **20**, 1947–1954, doi:10.1175/JCLI4095.1.
- Douglas, M. W., R. A. Maddox, K. Howard, and S. Reyes, 1993: The Mexican monsoon. *J. Climate*, **6**, 1665–1677, doi:10.1175/1520-0442(1993)006<1665:TMM>2.0.CO;2.
- Galarneau, T. J., Jr., L. F. Bosart, and A. R. Aiyer, 2008: Closed anticyclones of the subtropics and midlatitudes: A 54-yr climatology (1950–2003) and three case studies. *Synoptic–Dynamic Meteorology and Weather Analysis and Forecasting: A Tribute to Fred Sanders, Meteor. Monogr.*, No. 55, Amer. Meteor. Soc., 349–392.
- Higgins, W., and Coauthors, 2006: The NAME 2004 field campaign and modeling strategy. *Bull. Amer. Meteor. Soc.*, **87**, 79–94, doi:10.1175/BAMS-87-1-79.
- Hu, H., and F. Dominguez, 2015: Evaluation of oceanic and terrestrial sources of moisture for the North American monsoon using numerical models and precipitation stable isotopes. *J. Hydrometeor.*, **16**, 19–35, doi:10.1175/JHM-D-14-0073.1.
- Lavers, D. A., D. E. Waliser, F. M. Ralph, and M. D. Dettinger, 2016: Predictability of horizontal water vapor transport relative to precipitation: Enhancing situational awareness for forecasting western U.S. extreme precipitation and flooding. *Geophys. Res. Lett.*, **43**, 2275–2282, doi:10.1002/2016GL067765.
- Lin, Y., 2011: GCIPEOP Surface: Precipitation NCEP/EMC 4KM Gridded Data (GRIB) Stage IV data, version 1.0. UCAR/NCAR Earth Observing Laboratory, accessed 1 December 2015. [Available online at <http://data.eol.ucar.edu/dataset/21.093>.]
- Maddox, R. A., 1980: Mesoscale convective complexes. *Bull. Amer. Meteor. Soc.*, **61**, 1374–1387, doi:10.1175/1520-0477(1980)061<1374:MCC>2.0.CO;2.
- , D. M. McCollum, and K. W. Howard, 1995: Large-scale patterns associated with severe summertime thunderstorms over central Arizona. *Wea. Forecasting*, **10**, 763–778, doi:10.1175/1520-0434(1995)010<0763:LSPAWS>2.0.CO;2.
- Moore, B. J., P. J. Neiman, F. M. Ralph, and F. E. Barthold, 2012: Physical processes associated with heavy flooding rainfall in Nashville, Tennessee, and vicinity during 1–2 May 2010: The role of an atmospheric river and mesoscale convective systems. *Mon. Wea. Rev.*, **140**, 358–378, doi:10.1175/MWR-D-11-00126.1.
- Ralph, F. M., P. J. Neiman, G. A. Wick, S. I. Gutman, M. D. Dettinger, D. R. Cayan, and A. B. White, 2006: Flooding on California's Russian River: Role of atmospheric rivers. *Geophys. Res. Lett.*, **33**, L13801, doi:10.1029/2006GL026689.
- , and Coauthors, 2014: A vision for future observations for western U.S. extreme precipitation and flooding. *J. Contemp. Water Res. Educ.*, **153**, 16–32, doi:10.1111/j.1936-704X.2014.03176.x.
- , J. M. Cordeira, P. J. Neiman, and M. Hughes, 2016: Land-falling atmospheric rivers, the Sierra Barrier Jet, and extreme daily precipitation in northern California's upper Sacramento River watershed. *J. Hydrometeor.*, **17**, 1905–1914, doi:10.1175/JHM-D-15-0167.1.
- Rasmusson, E. M., 1967: Atmospheric water vapor transport and the water balance of North America. Part I: Characteristics of the water vapor flux field. *Mon. Wea. Rev.*, **95**, 403–426, doi:10.1175/1520-0493(1967)095<0403:AWVTAT>2.3.CO;2.
- Reitan, C. H., 1957: The role of precipitable water vapor in Arizona's summer rains. Tech. Rep. on the Meteorology and Climatology of Arid Regions 2, Institute of Atmospheric Physics, The University of Arizona, 19 pp. [Available from the Institute of Atmospheric Physics, The University of Arizona, Tucson, AZ 85721.]
- Saha, S., and Coauthors, 2010: The NCEP Climate Forecast System Reanalysis. *Bull. Amer. Meteor. Soc.*, **91**, 1015–1057, doi:10.1175/2010BAMS3001.1.
- , and Coauthors, 2014: The NCEP Climate Forecast System version 2. *J. Climate*, **27**, 2185–2208, doi:10.1175/JCLI-D-12-00823.1.
- Schmitz, J. T., and S. L. Mullen, 1996: Water vapor transport associated with the summertime North American monsoon as depicted by ECMWF analyses. *J. Climate*, **9**, 1621–1634, doi:10.1175/1520-0442(1996)009<1621:WVTAWT>2.0.CO;2.
- Sellers, W. D., and R. H. Hill, 1974: *Arizona Climate, 1931–1972*. The University of Arizona Press, 616 pp.
- Torn, R. D., and G. J. Hakim, 2008: Ensemble-based sensitivity analysis. *Mon. Wea. Rev.*, **136**, 663–677, doi:10.1175/2007MWR2132.1.
- , G. S. Romine, and T. J. Galarneau Jr., 2017: Sensitivity of dryline convection forecasts to upstream forecast errors for two weakly forced MPEX cases. *Mon. Wea. Rev.*, **145**, 1831–1852, doi:10.1175/MWR-D-16-0457.1.
- Ware, R. H., and Coauthors, 2000: SuomiNet: A real-time national GPS network for atmospheric research and education. *Bull. Amer. Meteor. Soc.*, **81**, 677–694, doi:10.1175/1520-0477(2000)081<0677:SARNGN>2.3.CO;2.
- Wilks, D. M., 1995: *Statistical Methods in the Atmospheric Sciences: An Introduction*. Academic Press, 467 pp.